11th World Congress on Computational Mechanics (WCCM XI)
5th European Conference on Computational Mechanics (ECCM V)
6th European Conference on Computational Fluid Dynamics (ECFD VI)
E. Oñate, J. Oliver and A. Huerta (Eds)

CAVITATION AND EVAPORATION IN METALS UNDER THE ACTION OF ULTRA-SHORT INTENSIVE IRRADIATION

POLINA N. MAYER* AND ALEXANDER E. MAYER*

* Chelyabinsk State University (CSU), Department of Physics
Bratyev Kashirinykh 129, 454001 Chelyabinsk, Russia
e-mail: polina.nik@mail.ru, mayer.al.evg@gmail.com

Key Words: *Cavitation, Evaporation, Metal, Intensive Irradiation, Two-Phase Medium.*

Abstract. We consider the dynamic fracture of metals in the liquid state as a non-equilibrium phase transition, consisting in nucleation and growth of spherical vapor cavities. Nucleation rate is obtained by the use of probability of corresponding thermal fluctuations; it accounts the work against surface tension. Governing equation for cavity growth accounts viscosity. The model treats irradiated metal as a two-phase medium which can be a singly connected liquid (solid) with (or without) vapor cavities–on the first stage of evolution; and a singly connected vapor with liquid drops–on the last stage. The resulting model is physically based and demands a minimum of fitting parameters; meanwhile it describes existing experimental and molecular dynamics results. The model allows calculating of the tensile strength of melts. It can be applied to the problem of intensive electron or laser irradiation of metals.

1 INTRODUCTION

Intensive ultra-short irradiation, electron, ion or laser, causes almost isochoric heating of substance and generates strong stresses in it [1,2]. Release of these stresses produces powerful tension of the material near irradiated and back surfaces of target due to the stress wave reflection. The tension leads to fracture and fragmentation, which can take place in the liquid state near the irradiated surface at a sufficient level of absorbed energy. Theoretical description of the dynamic fracture under described conditions is an important part of whole model of the substance behavior under intensive irradiation. Dynamic fracture of liquid metals is considered here as a non-equilibrium phase transition through formation, growth and coalescence of spherical cavities with accounting of substance evaporation on its surfaces.

2 MATHEMATICAL MODEL

In general case there are three phases in the irradiated substance: solid, liquid and vapor. Solid and liquid are considered as a single condensed phase in order to simplify the problem. Meanwhile, stress deviators are accounted for solid, and they are set to zero for liquid, as well as the shear modulus. The phase state (liquid or solid) of a condensed substance volume element can be found from a wide-range equation of state with phase boundaries tracking [3]. Vapor phase includes vapor cavities (bubbles) which are formed in the condensed phase undergoing fracture, although some of cavities are empty due to its small size and low vapor density. From this viewpoint the dynamic fracture is a non-equilibrium phase transition from condensed phase to vapor.

2.1 Substance dynamics

Dynamics of metal undergoing fracture is dynamics of a two-phase medium or mixture of the carrying agent and the disperse phase. The multiphase flow approach [4,5] is used, which is applicable if characteristic size of phase heterogeneities is much smaller than the scale of flow. The one-velocity approximation is also used, which means that both phases move with the same velocity. This velocity is determined by stresses in the carrying agent [4], and the motion equation takes the next form:

$$\rho \frac{d\upsilon_i}{dt} = -\frac{\partial P_{\mathrm{c}}}{\partial x_i} + \sum_{k=1}^{N} \frac{\partial S_{ik}}{\partial x_k}, \tag{1}$$

where υ_i is the velocity vector components; t is the time; x_k are the Cartesian coordinates; ρ is the substance density; P is the pressure and index ‘c’ means the carrying agent, while index ‘d’ will mean the dispersed phase; S_{ik} is the stress deviators (which are accounted only in the solid carrying agent); N is the number of dimensions of the considered problem, indexes i,k numerate the space directions. The total time derivatives are used in Eq. (1) and following equations, which are valid for Lagrangian particles moving with the substance.

Volume fractions of the carrying agent α_{c} and the disperse phase α_{d} can be found from the next equations:

$$\frac{d\alpha_{\mathrm{c}}}{dt} = \alpha_{\mathrm{d}} \sum_{k=1}^{N} \frac{\partial \upsilon_k}{\partial x_k} - w, \qquad \frac{d\alpha_{\mathrm{c}}}{dt} = -\alpha_{\mathrm{d}} \sum_{k=1}^{N} \frac{\partial \upsilon_k}{\partial x_k} + w, \tag{2}$$

where w is the growth rate of the dispersed phase volume per unit volume of mixture. True densities of phases ρ_c and ρ_d are used:

$$\frac{d\rho_{\mathrm{c}}}{dt} = \frac{\rho_{\mathrm{c}}}{\alpha_{\mathrm{c}}} \left(-\sum_{k=1}^{N} \frac{\partial \upsilon_k}{\partial x_k} + w \right) - \frac{J}{\alpha_{\mathrm{c}}}, \qquad \frac{d\rho_{\mathrm{d}}}{dt} = -\frac{\rho_{\mathrm{d}}}{\alpha_{\mathrm{d}}} w + \frac{J}{\alpha_{\mathrm{d}}}, \tag{3}$$

where J is the growth rate of the dispersed phase mass per unit volume of mixture. Change of internal energies, U_c and U_d, is governed by the next equations:

$$\alpha_{\mathrm{c}}\rho_{\mathrm{c}} \frac{dU_{\mathrm{c}}}{dt} = -P_{\mathrm{c}} \cdot \left(\sum_{k=1}^{N} \frac{\partial \upsilon_k}{\partial x_k} - w \right) - Q + \rho_{\mathrm{c}}\alpha_{\mathrm{c}} \cdot D - J \cdot \left(U_{\mathrm{tr}} - U_{\mathrm{c}} \right) + \sum_{k=1}^{N} \frac{\partial}{\partial x_k} \left(\kappa \frac{\partial T_{\mathrm{c}}}{\partial x_k} \right), \tag{4}$$

$$\alpha_{\mathrm{d}}\rho_{\mathrm{d}} \frac{dU_{\mathrm{d}}}{dt} = -P_{\mathrm{c}} \cdot w + Q + \rho_{\mathrm{d}}\alpha_{\mathrm{d}} \cdot D + J \cdot \left(U_{\mathrm{tr}} - U_{\mathrm{d}} \right),$$

where Q is the rate of heat exchange between phases per unit volume of mixture; D is the energy release function–the energy output by electron, ion or laser irradiation per unit mass of substance per unit time; U_{tr} is internal energy of the phase which mass is increasing; T_{c} is the temperature of the carrying agent and κ is the heat conductivity coefficient. The heat conductivity is accounted only for the carrying agent (see Eq. (4)).

Eqs (2)-(4) can be strictly derived from conservation of volume, mass and energy in a mixture element. Functions w, J and Q express the rates of exchange between phases, including phase transitions. Construction of the cavitation model is reduced to determination of these functions and it is considered in the following subsection. One should also determine pressure and stress deviators to obtain a closed system of equations. Pressure in each phase is connected with its true density and internal energy through the wide-range equation of state [3]. The elastic-plastic model [6,7] is used to determine the stress deviators in the solid phase; this model takes into account the dislocation dynamics and kinetics.

2.2 Cavitation in melt

Liquid is unstable against the liquid-vapor transition at pressure lower than the saturation vapor pressure; it happens when the liquid is expanded or overheated. The vapor pressure can not be less than zero; therefore, liquid at any negative pressure is unstable. Cavitation can occur in these conditions, which is formation and growth of vapor cavities. Formation of cavities demands the work against the surface tension; so, the liquid can exist as a metastable phase during some time [8].

Spherical shape of cavities is preferable due to the surface tension; change of its radius in viscous incompressible fluid is defined by the Rayleigh-Plesset equation [9,10]:

$$\ddot{R}_{(j)} = -\frac{3}{2}\frac{\dot{R}_{(j)}^2}{R_{(j)}} + \left[P_v - P_l - \frac{2\sigma}{R_{(j)}}\right]\cdot\frac{1}{R_{(j)}\,\rho_l} - \frac{8}{3}\frac{\eta}{\rho_l}\frac{\dot{R}_{(j)}}{R_{(j)}^2}, \qquad (5)$$

where indexes 'l' and 'v' indicates liquid (the melt) and vapor correspondently; σ is the coefficient of the surface tension; η is the coefficient of the melt viscosity; $R_{(j)}$ is the radius of cavity of j-th generation; dot on top denotes a time derivative.

The condition of cavity growth is $R > R_{\mathrm{cr}}$ where $R_{\mathrm{cr}} = 2\sigma/\left(P_v - P_l\right)$ is the critical radius. Formation of the critical cavity demands the next work: $W_{\mathrm{cr}} = \left(16\pi/3\right)\sigma^3/\left(P_v - P_l\right)^2$. Cavities can be nucleated due to thermal fluctuations. Such homogenous nucleation is a single opportunity if the liquid is uniform, like the melt of pure metal. The rate of homogenous nucleation of critical cavities is determined by the classical expression [10]:

$$\Pi = f\cdot n_a\cdot\exp\left(-\frac{W_{\mathrm{cr}}}{kT_l}\right)\cdot\alpha_l, \qquad (6)$$

where Π is the rate of cavities nucleation per unit mixture volume; n_a is the atoms concentration in the melt; f is the frequency factor, which is about $f \approx 10^{14}\ \mathrm{s}^{-1}$ according to the molecular dynamics (MD) simulations [11]. The critical work and the nucleation rate (6) depend nonlinearly on the surface tension coefficient, which is taken from [12].

Growth (5) and nucleation (6) can be simultaneous; therefore, all cavities are separated on groups or "generations" [13] according to the time of its formation: cavities of one generation were nucleated during a little time interval. Thus, the exchange rates of volume and mass can be written out as follows:

$$w = \frac{4\pi}{3} R_{\text{cr}}^3 \Pi + \sum_j \left(4\pi n_{(j)} R_{(j)}^2 \frac{dR_{(j)}}{dt} \right), \quad J = m_{\text{cr}} \Pi + \sum_j \left(n_{(j)} \frac{dm_{(j)}}{dt} \right). \tag{7}$$

where index j numerates generations; $n_{(j)}$ is the concentration of cavities of the corresponding generation. Growth rate of vapor mass in cavity can be obtained [14] from the theory of phase transitions.

Growing cavities can coalescence and form a singly-connected vapor phase, which is accompanied by the liquid fragmentation on drops–it is the complete fracture. It is supposed that the complete fracture takes place in a mixture element when the volume fraction of vapor ranks over one half. Then the carrying agent and the dispersed phase change over in this element, dynamics are described by similar, but slightly different equations.

3 NUMERICAL IMPLEMENTATION

The described above cavitation model is numerically realized in CRS computer program in 1D and 2D cases. This program is designed to simulate various intensive actions on metal: high-speed impact, intensive electron, ion and laser irradiation.

Method of separation by physical processes is used with the next subproblems: 1) substance dynamics (Eqs. (1)-(3)); 2) melt tracking and dislocation plasticity in solid part of the metal; 3) cavitation and evaporation in overheated (or expanded) melt. Equations for all these processes are solved independently on each time step, and the data exchange takes place at the end of each step. Subproblem of the substance dynamics are solved by modification of the numerical method [15]. Modification consists in eliminating of artificial viscosity and accounting of the physical viscosity instead; it allows to obtain the stable numerical solution by using of a fine enough computational grid [16]. All other equations are solved by the Euler method with a varied time step.

4 CALCULATION RESULTS

4.1 Dynamic strength of metal melts

Fig. 1 shows results for uniform tension of aluminum melt in comparison with the experimental and MD data. Surface tension coefficients for melt and heir temperature dependences are taken from [12]. The negative pressure increases with tension at first; then the metal loses its strength due to cavitation and the pressure falls (Fig. 1(a)). Further tension leads to a complete fracture with the condensed phase fragmentation on drops; maximal negative pressure is the dynamic tensile strength. Homogenous nucleation is dominant in the melt; tensile strength of melt slowly increases with the strain rate increase and rapidly decreases with the temperature growth (Fig. 1(b)); meanwhile, the fragments size (drops diameter) decreases in inverse proportion to the strain rate: from about 0.1 mm at 10^5 s^{-1} down to about 10 nm at 10 s^{-1}.

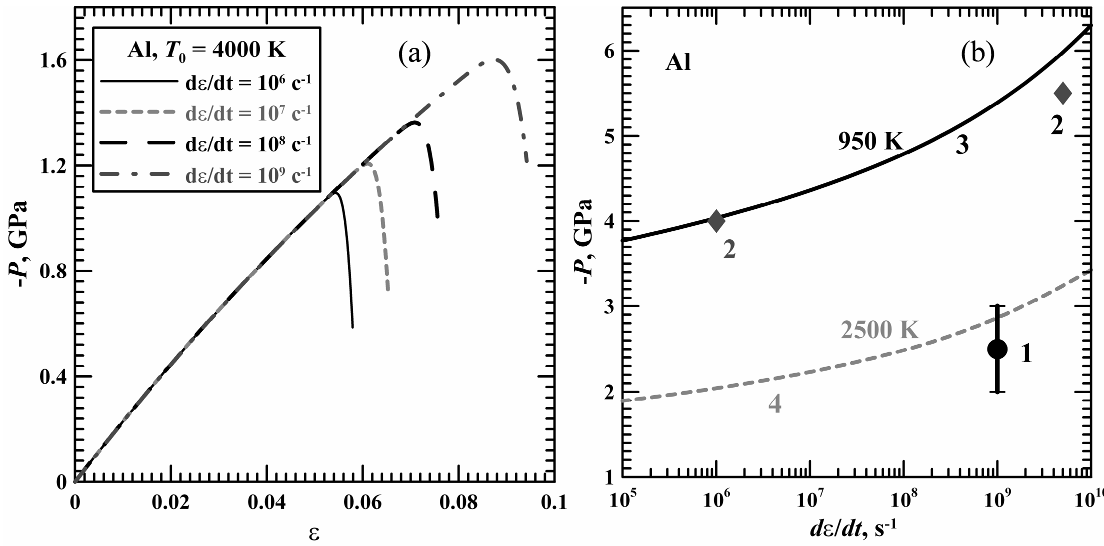

Figure 1: Dynamic fracture at uniform tension of the aluminum melt: (a) pressure versus current strain; (b) maximal achieved negative pressure (dynamic tensile strength) versus strain rate at deferent temperatures; markers: 1-the experimental result [17]; 2-the MD simulations [11] for corresponding temperatures.

4.2 High current electron irradiation

Here we numerically investigate the copper irradiation by the high-current pulsed electron beam with parameters: the energy of fast electrons is 1 MeV, the beam current density is 10 kA/cm^2, the pulse duration is 50 ns. The beam action causes the sharp, almost isochoric, heating of the substance (up to 2700 K) in the energy release zone (Fig. 2, left panel) and the formation of area of the high-pressure–up to 11 GPa (Fig. 2, right panel). The substance temperature exceeds the melting temperature up to the depth of 0.4 mm; in this layer the metal is melted. Release of the high pressure area results in formation of the compression wave with the amplitude of about 6 GPa. The compression wave front is becoming sharper with the time, and it transforms into the shock wave. Reflection from the free (irradiated) surface forms the tensile wave, following behind the shock wave. This tensile wave creates the negative pressure with the value up to 3.5 GPa in the liquid metal, which initiates the fracture of the liquid phase through cavitation. The generation and growth of cavities result in a reduction of the liquid metal volume and, therefore, it decreases the tensile stresses due to the substance compression; the substance passes in the equilibrium two-phase state. This process restricts the tensile stresses; otherwise, the rarefaction wave amplitude would be the same as the amplitude of the compression wave. Irradiation is from the left free surface in all figures.

It should be noted that the existence of a metastable liquid state leads to propagation of the tensile wave inside the metal behind the shock wave. Negative pressure in this tensile wave can reach the value of the dynamical strength, 3.5 GPa. Thus, the structure of stresses in metal differs from that in calculations [18], where the approximation of liquid-vapor equilibrium was used for the melted part of the metal. Tensile wave can substantially influence on the material modification [19] as well as on the spall fracture of solid metal near its back surface.

Cavitation leads to decrease of volume fraction of the condensed phase (Fig. 3, left panel) and to decrease of the average density of mixture (Fig. 3, right panel). Cavitation does not touch the surface layer–tensile stresses here is too little; therefore, a layer of condenced metal melt is spelled due to the cavitation in full analogy with the back-side spallation of solids.

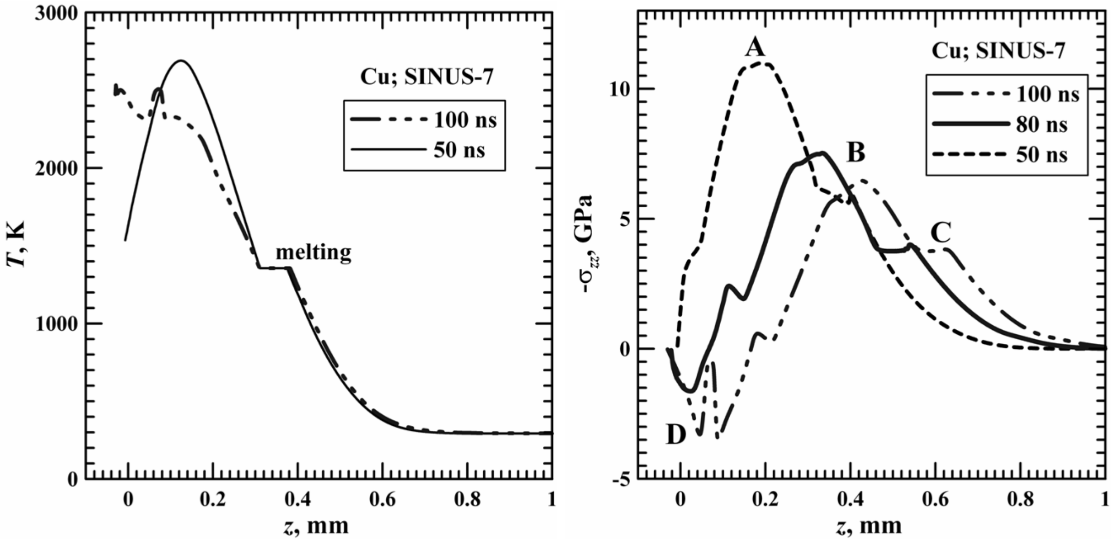

Figure 2: Temperature (left panel) and stress (right panel) fields in copper under the action of high-current electron irradiation with parameters, corresponding to SINUS-7 accelerator [1]. "A"–the high pressure zone; "B"–the running stress wave with elastic precursor "C"; "D"–cavitation zone in melt as a result of its tension.

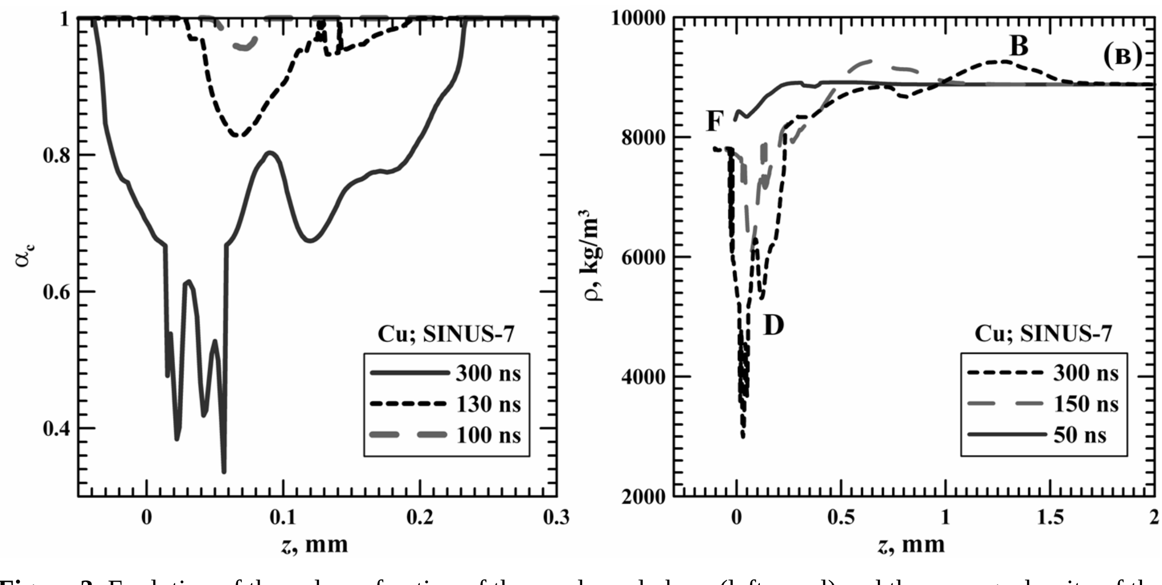

Figure 3: Evolution of the volume fraction of the condensed phase (left panel) and the average density of the mixture (right panel) in copper under the action of the high-current electron irradiation with parameters, corresponding to SINUS-7 accelerator [1]. "F"–spalled liquid layer; "B"–the running stress wave; "D"–cavitation zone in the melt.

The model can predict the sizes of metal particles ablated from the irradiated surface (see Fig. 4). These particles are formed after complete fracture of the melt due to coalescence of cavities and then undergo solidification. Smallest particles are formed near the centre of the energy release zone, while the largest one–new the boundaries of the cavitation zone. As a result, the size distribution of all formed particles is wide. Typical size is of the order of several tens of micrometers in the considered case.

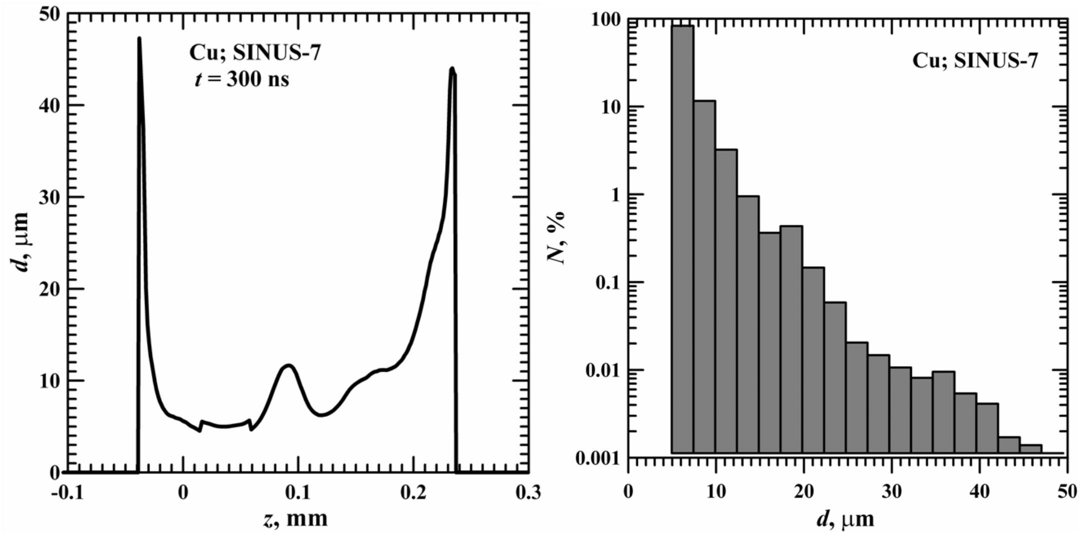

Figure 4: Average size of metal particles versus coordinate (left panel) and histogram of size distribution of particles collected over all depth of the ablation zone (right panel). Copper, high-current electron irradiation with parameters, corresponding to SINUS-7 accelerator [1].

5 CONCLUSIONS

- Computational model of cavitation and evaporation of the irradiated metal is described. The model considers substance as a two-phase mixture (condensed phase + vapor) with mass, volume and energy exchange between phases.
- The model allows to calculate the dynamic tensile strength of melts without any additional model parameters besides of the surface tension coefficient, which is already available in literature. These calculations correspond to available experimental data on ultra-short pulse laser irradiation of thin metal foils.
- Metal ablation in the energy-release zone of the high-current pulsed electron beam is investigated on the basis of the proposed model. Simulations detect the formation of spalled liquid layer on the irradiated surface, which is followed bymixture of metal drops and vapor. This mixture is formed in the cavitation zone due to coalescence of vapor cavities. Typical size of drops is of about several tens of micrometers.
- The metastable state of metal melt influence substantially on the stress fields and modification processes in the solid part of the metal.

This work is supported by the Russian Foundation for Basic Research (Grant No. 14-01-31454) and by grant of the President of Russian Federation (MD-286.2014.1).

REFERENCES

[1] Dudarev, E.F., Kashin, O.A., Markov, A.B., Mayer, A.E., et al. Deformation behavior and spalling fracture of a heterophase aluminum alloy with ultrafine-grained and coarse-

grained structure subjected to a nanosecond relativistic high-current electron beam. Russ. Phys. J. (2011) **54**:713-720.

[2] Inogamov, N.A., Zhakhovsky, V.V., Petrov, Yu.V. et al. Electron-Ion Relaxation, Phase Transitions, and Surface Nano-Structuring Produced by Ultrashort Laser Pulses in Metals. *Contrib. Plasma Phys.* (2013) **53**:796-810.

[3] Fortov, V.E., Khishchenko, K.V., Levashov, P.R. and Lomonosov, I.V. Wide-range multi-phase equations of state for metals. *Nucl. Instrum. Meth. Phys. Res. A* (1998) **415**:604-608.

[4] Nigmatulin, R.I. *Dynamics of Multiphase Media*. Hemisphera PC, New York, (1990).

[5] Van Wachem, B.G.M. and Almstedt, A.E. Methods for multiphase computational fluid dynamics. *Chem. Engng J.* (2003) **96**:81-98.

[6] Krasnikov, V.S., Mayer, A.E. and Yalovets, A.P. Dislocation based high-rate plasticity model and its application to plate-impact and ultra short electron irradiation simulations. *Int. J. Plast.* (2011) **27**:1294-1308.

[7] Mayer, A.E., Khishchenko, K.V., Levashov, P.R. and Mayer, P.N. Modeling of plasticity and fracture of metals at shock loading. *J. Appl. Phys.* (2013) **113**:193508.

[8] Skripov, V.P. *Metastable Liquids*. Wiley, New York, (1974).

[9] Brennen, C. *Cavitation and Bubble Dynamics*. Oxford University Press, New York (1995).

[10] Kuksin, A.Yu., Norman, G.E., Pisarev, V.V., et al. Theory and molecular dynamics modeling of spall fracture in liquids. *Phys. Rev. B* (2010) **82**:174101.

[11] Kuksin, A.Yu., Levashov, P.R., Pisarev, V.V., et al. Model of fracture of liquid aluminum based on atomistic simulations. *Physics of Extreme States of Matter-2011*. IPCP RAS, Chernogolovka, (2011):57-59.

[12] Lu, H.M. and Jiang, Q. Surface tension and its temperature coefficient for liquid metals. *J. Phy. Chem. B* (2005) **109**:15463-15468.

[13] Volkov, N.B., Fen'ko, E.L. and Yalovets, A.P. Simulation of generation of ultradisperse particles upon irradiation of metals by a high-power electron beam. *Techn. Phys.* (2010) **55**:1389-1399.

[14] Mayer, P.N. and Mayer, A.E. Droplet size distribution in a metal evaporated by high-current electron beam. *Techn. Phys. Let.* (2012) **38**:559-561.

[15] Yalovets, A.P. Calculation of flows of a medium induced by high-power beams of charged particles. *J. Appl. Mech. Tech. Phys.* (1997) **38**:137–150.

[16] Mayer, A.E. and Khishchenko, K.V. Numerical study of shock-wave structure in elastic-plastic medium. *Physics of Extreme States of Matter–2014*. JIHT RAS, Moscow, (2014):45-48.

[17] Ashitkov, S.I., Komarov, P.S., Ovchinnikov, A.V., et al. Femtosecond laser ablation and strength of liquid metals at extremely high extension rates. *Scientific-Coordination Session on Non-Ideal Plasma Physics.* JIHT of RAS, Moscow, (2012).

[18] Chistyakov, S.A., Khalikov, S.V. and Yalovets, A.P. Investigation of the formation of elastoplastic waves in a metal target irradiated with charged particles. *Techn. Phys.* (1993) **38**:5-9.

[19] Krasnikov, V.S. and Mayer, A.E. Numerical investigation of the change of dislocation density and microhardness in surface layer of iron targets under the high power ion- and electron-beam treatment. *Surf. Coat. Techn.* (2012) **212**:79-87.